Preprints of the 19th World Congress
The International Federation of Automatic Control
Cape Town, South Africa. August 24-29, 2014

# A modified polynomial-based controller for enhancing the positioning bandwidth of nanopositioners.

**Mohammad Namavar** * **Sumeet S. Aphale** *

* *Centre for Applied Dynamics Research, School of Engineering, University of Aberdeen, UK*

**Abstract:** Polynomial-based damping techniques such as Positive Position Feedback (PPF) and Positive Velocity and Position Feedback (PVPF) have been applied successfully to a number of lightly damped systems to overcome resonance-induced vibration issues. These control designs exhibit several advantages such as substantial damping performance, relative ease of design and adequate robustness in the presence of plant parameter uncertainties. Their formulation is based on the well-known pole-placement technique where damping is achieved by pushing the poles of the close-loop system arbitrarily away from the $j\omega$ axis and in to the left-half plane. Current designs result in changing the real part of the poles while keeping the imaginary part unaltered; thus keeping the resonant frequency of the closed-loop, damped system unchanged, compared to the original undamped, open-loop system. In this work, we present a pole-placement technique which results not only in the substantial damping of the resonance but also in shifting the system resonance to a substantially higher frequency. This result is beneficial to a number of systems such as nanopositioners employed in Scanning Probe Microscopes, where maximizing the positioning bandwidth is a major goal and the achievable bandwidth is severely limited by the resonant frequency of the positioner.

## 1. INTRODUCTION

Unwanted vibration due to excitation of system resonance is one of the main performance limiting factors in many technological systems Preumont (2002). Nanopositioners are a small but important class of systems which suffer from resonance-related issues such as positioning errors and fatigue. Additionally, as most nanopositioners employ some form of piezoelectric actuator, they are also marred by inherent piezoelectric nonlinear effects such as hysteresis and creep. The most prevalent method to overcome these problems and improve the positioning performance of nanopositioners is to adopt a hybrid control scheme that combines a suitably designed damping controller with some type of tracking control Fleming and Wills (2009).

Piezoelectric-tube nanopositioners or piezo-stack actuated platform nanopositioners employed in Scanning Probe Microscopes (SPM), possess a low-pass frequency response characteristic dominated by a single, lightly-damped resonant mode evident at relatively low frequencies ($< 1$ KHz). Consequently, their frequency response measured from output displacement to input positioning command can be accurately modeled as a lightly-damped second-order transfer function. Nanopositioners are routinely employed as positioning platforms for Atomic Force Microscopes (AFM) and are required to be able to trace a raster pattern which can be generated by combining the motion of two axes of a platform where one axis traces a triangular path and the other axis traces a slow ramp Devasia et al. (2007). As the triangle waveform comprises of infinite odd harmonics of the fundamental frequency, the lightly-damped resonance of the nanopositioner can be excited by one of the triangle waveform's higher harmonic components and result in substantial positioning errors Fleming and Wills (2009). Thus, if the nanopositioner is to be utilized as is (undamped, open-loop), the triangle wave frequency is generally limited to less than $1/100^{th}$ the frequency of the resonance Fleming and Wills (2009). These slow scan speeds are inadequate for scanning samples that change over time (cell-biology) Zou et al. (2004). To improve the positioning performance of the nanopositioner (and ultimately the AFM / SPM employing it), closed-loop schemes that damp the system resonance and track the input triangle accurately are routinely employed Devasia et al. (2007). The key performance criteria for nanopositioning applications then is positioning bandwidth, i.e., a range of frequencies (0 Hz - $f_{max}$ Hz) within which the positioning errors lie within an acceptable limit.

A number of active control techniques have been formulated to enhance the positioning performance of these nanopositioners Moheimani (2003); Aphale et al. (2007); Preumont (2002); Salapaka et al. (2002); Fanson and Caughey (1990); Bhikkaji et al. (2007); Pota et al. (2002). Polynomial-based pole-placement controller is one of the popular techniques that has shown the ability to impart substantial damping to lightly-damped resonant modes Goodwin et al. (2001). This technique has been applied to nanopositioning tubes Bhikkaji et al. (2007) and platforms Aphale et al. (2008) successfully and has mainly been presented in three distinct flavors viz: Positive Velocity and Position Feedback (PVPF) also known as polynomial-based controller Bhikkaji et al. (2007), Positive Position Feedback (PPF) Ratnam et al. (2005) and Resonant controller Pota et al. (2002). The main advantages of a

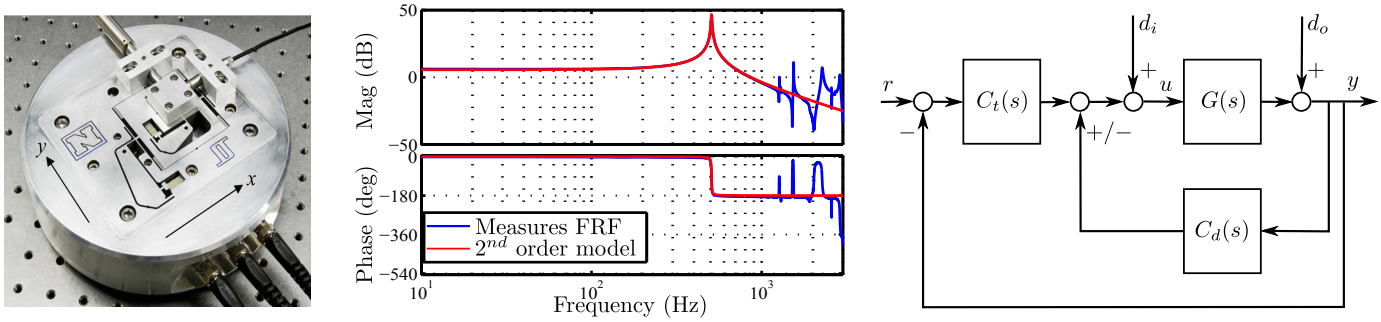


(a) (b) (c)

Fig. 1. (a) Multi-Axis Serial-Kinematic Nanopositioner designed at EasyLab, University of Nevada-Reno. (b) Measured frequency response of the nanopositioner (blue) along with second-order model (red) used for controller design. (c) Block diagram shows the control scheme for damping and tracking control. Damping controller $C_d(s)$ is either implemented in positive or negative feedback and damps the resonant peak. Tracking controller $C_t(s)$ is usually an integral controller implemented in negative feedback.

polynomial-based controller are: substantial damping performance, relative ease of design and adequate robustness in the presence of plant parameter uncertainties. The design is based on the well-known pole-placement technique where damping is achieved by pushing the poles of the close-loop system arbitrarily away from the $j\omega$ axis and further in to the left-half plane Fanson and Caughey (1990). All the designs reported so far change the real part of the poles, thus keeping the resonant frequency of the closed-loop, damped system unaltered compared to the original undamped, open-loop system. Though adequate damping is achieved by such manipulation, the positioning bandwidth remains limited by the nominal resonance frequency of the nanopositioner.

It was generally accepted that increasing the positioning bandwidth of a given nanopositioner would basically enforce a mechanical redesign that results in a resonance at a higher frequency. Recently Namavar et al. (July, 2013), it was shown that closed-loop control could be effectively employed to not only deliver adequate damping but also shift the resonance frequency of the overall system, thereby resulting in substantial increase in positioning bandwidth. In this work, we utilize the flexibility afforded by the polynomial-based controller technique to not only damp the resonance but also push the system resonance to a higher frequency. This resonance-enhanced damping scheme combined with a suitable tracking controller (an integrator) delivers a substantial increase in the overall positioning bandwidth. Furthermore, it is shown that this technique also exhibits superior input-disturbance rejection characteristics when compared to the traditional polynomial-based designs.

This paper is structured as follows. In Section 2, the system model, the damping controller and the tracking controller are briefly described. Section 3 explains the modified controller design approach and is followed by simulation results presented in Section 4. A detailed comparison between the traditional polynomial-based controller (PBC) performance and the modified polynomial-based controller (MPBC) performance is presented, clearly demonstrating the key performance advantages delivered by the modified design. Section 5 concludes the paper.

## 2. BACKGROUND

### 2.1 System Model

As described earlier, the frequency-response of a typical nanopositioner measured from output displacement of one axis to input command signal to the same axis shows the presence of a dominant lightly-damped resonant mode Aphale et al. (2008). In most cases, the dynamics beyond the first resonant mode roll-off quickly and can be (and usually are) neglected; therefore the useful model of an axis of the nanopositioner reduces to a lightly-damped second-order transfer function with a feed-through term added to compensate for the truncation of the high-frequency response data Moheimani (2000). This can be given by:

$$G(s) = \frac{\alpha}{s^2 + 2\xi\omega_n s + \omega_n^2} + d, \tag{1}$$

where $\xi$, $\omega_n$, and $d$ are damping ratio, undamped natural frequency, and the feed-through term respectively. Here, $\alpha = dc_{gain} \times \omega_n^2$.

### 2.2 Traditional Control Design

*Damping Controller* Aphale et al. (2008) presents a detailed comparison of the damping imparted to the dominant resonant mode of a nanopositioner by three popular controllers viz: (i) Polynomial-based Controller, (ii) Positive Position Feedback (PPF) and (iii) Resonant Control. Based on the simulations as well as the experimental results, it was concluded that the Polynomial-based Controller (PBC) resulted in the best overall performance in terms of damping and disturbance rejection. Additionally, in conjunction with a suitably designed integral tracking controller, it was shown to deliver the best positioning performance Aphale et al. (2008). The strategy of designing the polynomial-based controller is to move the lightly-damped poles of the resonant system further into the left-half plane (LHP), thereby imparting substantial damping to them. The resulting controller is a second-order transfer-function given by:

$$C_d(s) = \frac{\Gamma_1 s + \Gamma_2}{s^2 + 2\delta\omega_p s + \omega_p^2} \tag{2}$$

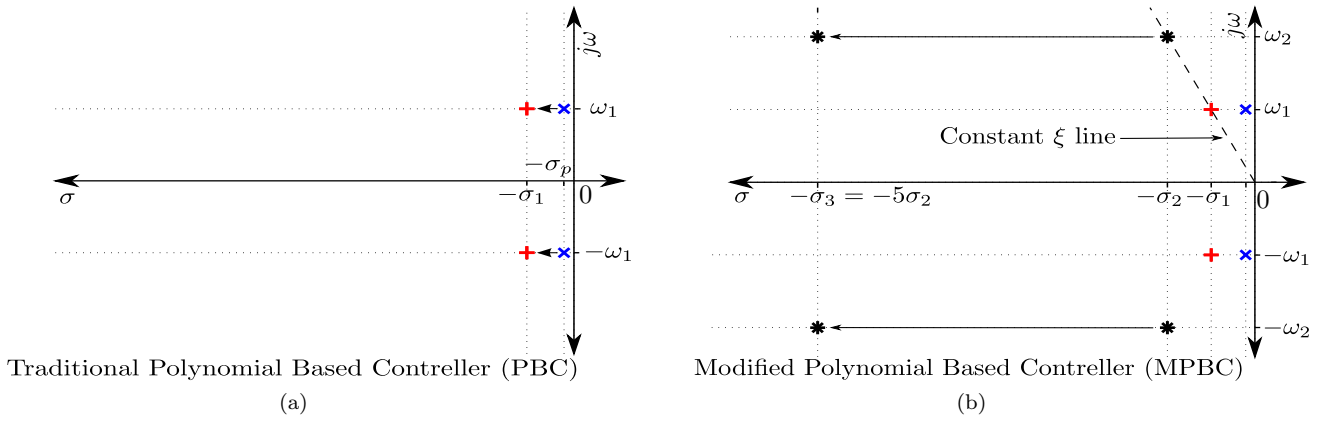


Fig. 2. (a) Open-loop poles of the nanopositioner are shown as blue ×. Closed-loop implementation of the traditional PBC results in shifting the poles (denoted by red +) further into the left half plane, resulting in resonance damping. (b) The placement of the system poles as a result of the MPBC implementation (denoted by black ∗) clearly shows the location of poles compared to that achieved by the PBC.

*Tracking Controller* For nanopositioning applications, a tracking controller is implemented to ensure that the output $y$ follows the desired reference input $r$ with high accuracy. The source of error can either be external disturbances and / or nonlinearities of the piezoelectric actuators namely: hysteresis and creep. A suitably gained integrator given by (3) is generally utilized.

$$C_t(s) = \frac{k_t}{s} \tag{3}$$

A block-diagram of the overall control scheme is shown in Fig. 1(c). The tracking gain $k_t$ is determined by different performance criteria such as maximum tracking bandwidth and minimum settling time. In Section 3, both cases are discussed.

## 3. MODIFIED POLYNOMIAL-BASED CONTROLLER DESIGN (MPBC)

Traditional PBC design focuses on damping the resonant mode by pushing the poles further into the left-half plane (LHP) while keeping the resonant frequency unchanged ($j\omega$ coordinate of the poles is unchanged) Aphale et al. (2008); Yong et al. (2009); Bhikkaji et al. (2007). In the *Modified Polynomial-based Controller* (MPBC) approach we aim to place the closed-loop poles in the $s$-plane such that both the real as well as the imaginary coordinates of the poles are changed; thereby increasing the resonant frequency ($\omega_n$) as well as the damping coefficient ($\xi$).

The generic transfer-function of the PBC is given by (2) and consists of two poles and one zero, implemented in a positive feedback loop. Controller parameters are $\Gamma_1, \Gamma_2, \delta$ and $\omega_p$. The resulting closed-loop transfer function of the damped system $G_d(s)$ is:

$$G_d(s) = \frac{G(s)}{1 - G(s)C_d(s)}, \tag{4}$$

where its poles are the roots of $P(s)$, see (5).

$$\begin{aligned} P(s) = s^4 &+ (2\xi\omega_n + 2\delta\omega_p)s^3 \\ &+ (\omega_n^2 + 2\xi\omega_n * 2\delta\omega_p + \omega_p^2)s^2 \\ &+ (2\xi\omega_n\omega_p^2 + 2\omega_n^2\delta\omega_p - \alpha\Gamma_1) \\ &+ \omega_n^2\omega_p^2 - \alpha\Gamma_2 \end{aligned} \tag{5}$$

**Note**: Since the closed-loop poles will be placed arbitrarily in the LHP, feed-through term $d$ can be neglected.
Assume the desired closed-loop poles are the roots of $Q(s)$, see (6).

$$Q(s) = s^4 + K_1 s^3 + K_2 s^2 + K_3 s + K_4 \tag{6}$$

Controller parameters are determined by solving a set of four simultaneous equations by matching the coefficients of $P(s)$ and $Q(s)$ for the same power of $s$. A mathematical approach to designing such a controller is reported in Bhikkaji et al. (2007). It is shown that the amount of pole displacement with respect to $j\omega$ axis is not restricted theoretically as long as the conditions defined in Bhikkaji et al. (2007) are satisfied. However, there are some practical limitations such as required control effort and disturbance rejection capabilities.

In the MPBC design, we assume that the amount of damping imparted by the traditional PBC suits the application and the MPBC is designed to impart the same amount. To achieve same amount of damping as imparted by the traditional PBC, one pair of closed-loop poles is placed on the straight line passing through origin and the traditional PBC poles (the constant $\xi$ line) such that the frequency of the closed-loop poles greater than the open-loop poles of the system, see Fig. 2. The other pair is placed at the same $j\omega$-coordinate as the first pair but five times further in to the LHP. Such pole-placement has shown to effectively reduce the adverse effects on the closed-loop transfer function Dorf and Bishop (2010). The resulting fourth-order closed-loop transfer function exhibits a substantially damped resonant mode. If both closed-loop pairs are placed at the same location (at the higher $j\omega$ coordinate), it was found that the overall closed-loop system behaves like an under-damped system. A detailed comparison of the improvements afforded by the proposed

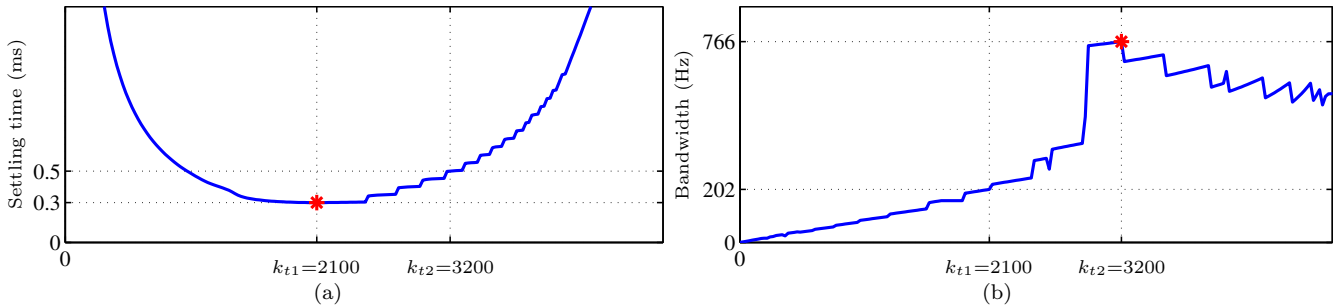


Fig. 3. Numerical optimization for tracking gain selection: (a) shows that $K_{t1} = 2100$ is the best choice for minimum settling time for overall closed-loop system. (b) shows the suitable gain for maximizing $\pm 1$ dB bandwidth is $K_{t1} = 3200$.

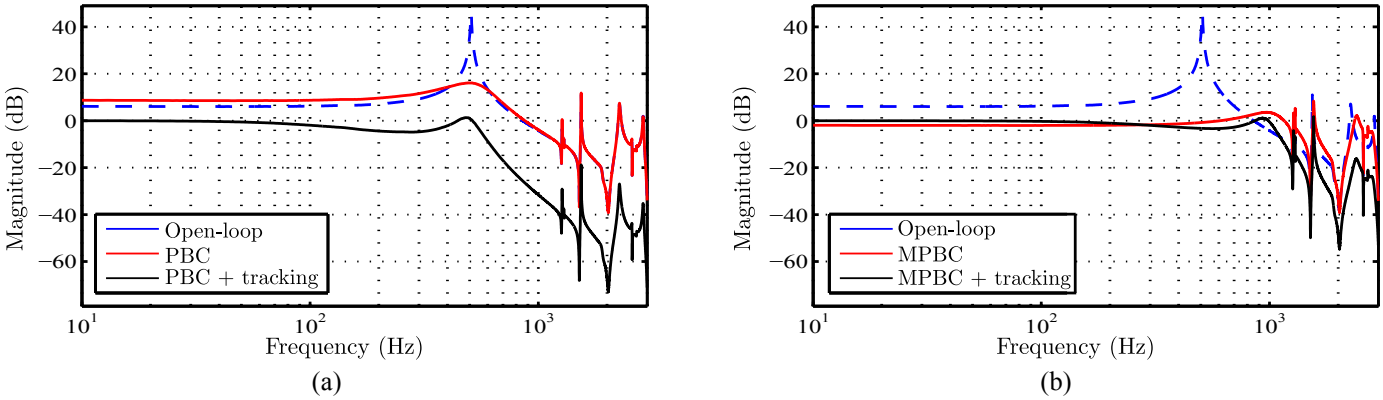


Fig. 4. (a) Open-loop (dashed blue), traditional PBC (red), and TPBC plus tracking controller(black). (b) Open-loop (dashed blue), MPBC (red), and MPBC plus tracking controller (black).

MPBC over the traditional PBC is presented in the next section.

## 4. SIMULATION RESULTS

### *4.1 System Model*

The second-order transfer-function that accurately models the frequency response of one axis of a nanopositioning platform shown in Fig. 1 is given by:

$$G(s) = \frac{1.925 \times 10^7}{s^2 + 27.74s + 1.016 \times 10^7} \tag{7}$$

The dominant resonant mode occurs at 507 Hz and has a magnitude of 46.8 dB. The system has two stable, underdamped complex conjugate poles at $-13.9 \pm j3187.4$.

### *4.2 Damping Controller*

In the traditional PBC design, it was seen that adequate damping was achieved by placing the closed-loop poles a 1000 units further into the LHP, resulting in two complex conjugate pairs at $-1014 \pm j3187$. For the MPBC, one pole-pair was placed at $-2028 \pm j6375$. This placement imparted the same damping to the system as the traditional PBC but effectively increased the system resonance by two times. The other pair was placed at $(-5 \times 2028) \pm j6375$. The resulting MPBC transfer-function is given by:

$$C_{dm}(s) = \frac{-6.42 \times 10^4 s - 1.96 \times 10^8}{s^2 + 2.43 \times 10^4 s + 2.60 \times 10^8} \tag{8}$$

### *4.3 Tracking Controller*

To determine the tracking controller gain $k_t$, a numerical search was carried out to identify the optimal gain for two important performance criteria namely: (i) Maximum tracking bandwidth and (ii) Minimum settling time. The appropriate gain that minimized the settling time of the overall closed loop system was found to be $k_{t1} = 2100$, see Fig. 3a.

A convincing argument pointing out the inadequacies of applying the well-known criteria of $-3$ dB bandwidth criteria to nanopositioning systems has been detailed in Namavar et al. ((in press). Therefore, a $\pm 1$ dB bandwidth criteria was employed. The corresponding gain, $k_t$, which maximizes the tracking bandwidth was numerically searched and found to be $k_{t2} = 3200$, see Fig. 3b.

### *4.4 Results*

Frequency responses for open-loop, damped closed-loop as well as damped and tracked closed-loop for the traditional PBC as well as the MPBC are given in Fig. 4(a) and Fig. 4(b) respectively. Parametric comparison of both the techniques has been tabulated in Table (1). As reported, the MPBC technique results in a $\pm$ 1 dB positioning bandwidth of 200 Hz which is almost 2.5 times that achieved by the traditional PBC technique (70 Hz). -3 dB bandwidth shows an increase of more than three times with the MPBC implementation.

Table 1. Parametric comparison between the traditional Polynomial-based controller and the proposed MPBC

| Parameter | For Traditional PBC | For proposed MPBC |
|---|---|---|
| Damping controller $C_d(s)$ | $C_{dt}(s) = \frac{-208s+2.06\times10^6}{s^2+4028s+1.62\times10^7}$ | $C_{dm}(s) = \frac{-6.42\times10^4 s-1.96\times10^8}{s^2+2.43\times10^4 s+2.60\times10^8}$ |
| Damped system poles | 2 pairs at $-1014 \pm j3187$ | $-2028 \pm j6375$ and $-10116 \pm j6375$ |
| Tracking controller $C_t(s)$ | $C_{tt} = \frac{260}{s}$ | $C_{tm} = \frac{2100}{s}$ |
| Settling Time (ms) | 7.1 | 2.5 |
| $\pm$1 dB Bandwidth (Hz) | 70 | 200 |
| -3 dB Bandwidth (Hz) | 143 | 440 |
| RMS Error (20 Hz, 2 $\mu$m) | 0.109 | 0.047 |
| RMS Error (40 Hz, 2 $\mu$m) | 0.207 | 0.093 |

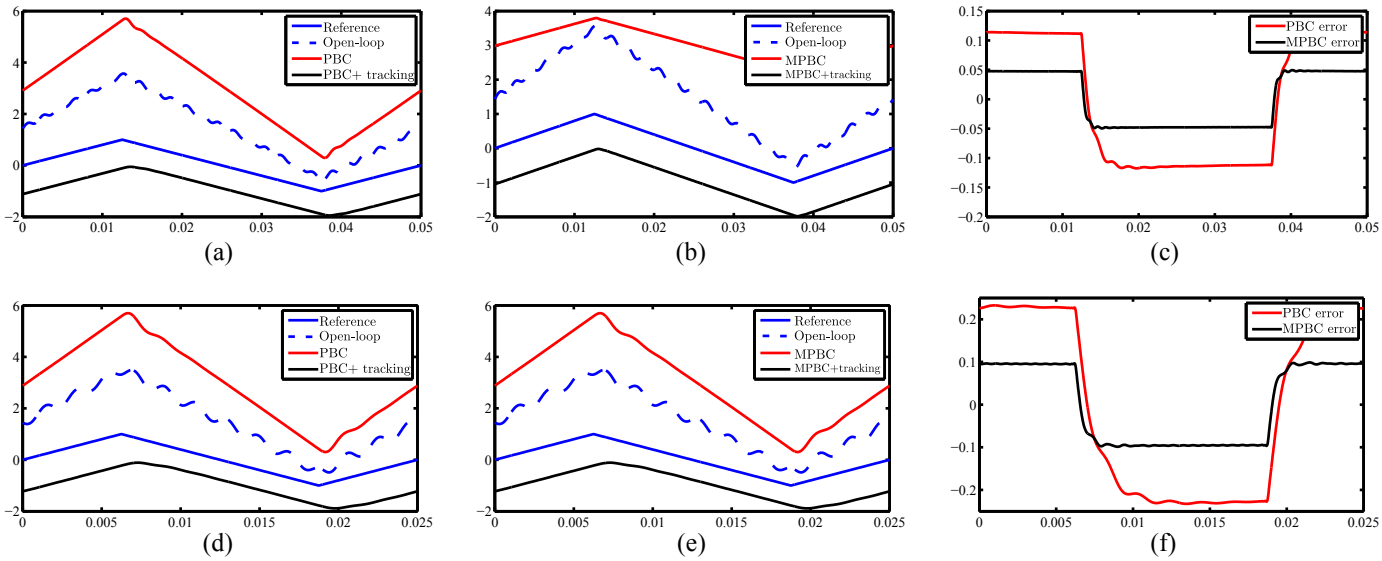


Fig. 5. (a) and (d) Time-domain traces generated by the PBC-based closed-loop system for 20 Hz and 40 Hz triangular inputs respectively. (b) and (e) Time-domain traces generated by the MPBC-based closed-loop system for 20 Hz and 40 Hz triangular inputs respectively. (c) and (f) Error plots for the PBC-based and MPBC-based closed-loop system for 20 Hz and 40 Hz triangular inputs respectively. Note that in (a), (b), (d) and (e) signals are shifted vertically for clarity.

Positioning performance for both the PBC-based as well as the MPBC-based closed-loop systems was simulated using triangular positioning commands at $f_1 = 20$ Hz and $f_2 = 40$ Hz. These time-domain results are presented in Fig. 5. As seen from Fig. 5(c) and (f) and reported in Table (1), the MPBC-based closed-loop system reduces positioning errors to less than 50% of those produced by the PBC-based closed-loop system.

### *4.5 Disturbance rejection characteristics*

Input disturbance and measurement noise (sensor noise) are common causes for positioning errors. Transfer functions from output to input disturbance ($y(s)/d_i(s)$) as well as from output to measurement noise ($y(s)/d_o(s)$) were computed (using Fig. 1(c)) and their frequency-responses were analyzed. Fig. 6(a) shows that the MPBC scheme exhibits superior input disturbance rejection characteristics compared to the traditional PBC scheme.

Measurement noise is an inherent characteristic of using closed-loop techniques. Fig. 6(b) shows that the PBC scheme closed-loop rolls off sooner than the one employing the MPBC. As most position sensors exhibit low-pass characteristics and come equipped with an adjustable cutoff, this is not a major drawback.

## 5. CONCLUSIONS

The modified polynomial-based controller design (MPBC) results in a controller with the potential to significantly increase the positioning bandwidth of the overall damped and tracked system without the need of any physical modifications to the nanopositioner. The simulation results show that MPBC increased the positioning bandwidth by 2.85 times and provided a significantly improved input disturbance rejection capability. Though the traditional polynomial-based controller (PBC) scheme has better output disturbance rejection characteristics, the significant increase in positioning bandwidth as well as the improved input disturbance rejection afforded by the MPBC deems the proposed design modification beneficial to nanopositioning and similar precision positioning applications. Experimental verification, mathematical optimization of tracking gains as well as further refinements to the pole-placement strategy are currently in progress.

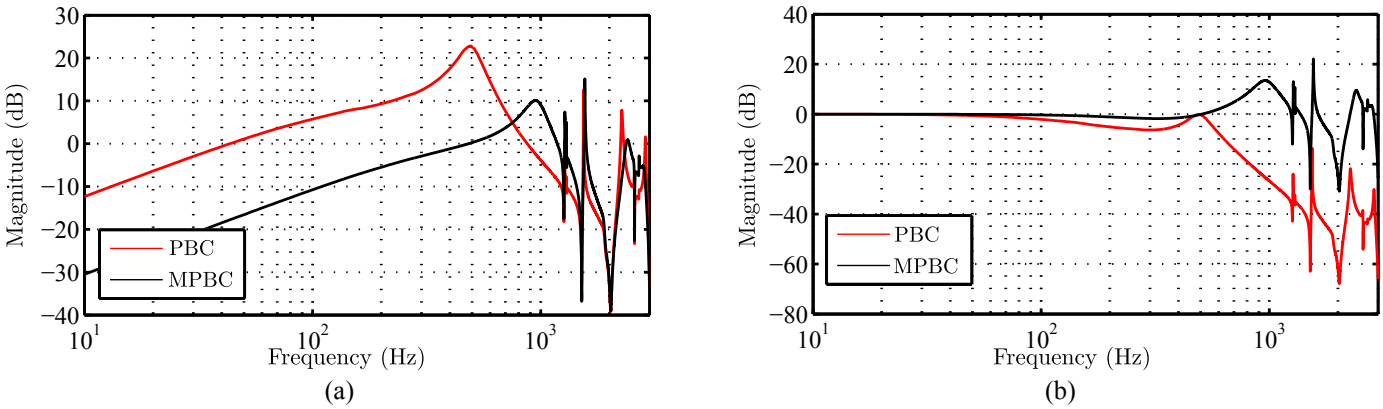


Fig. 6. (a) Output to input disturbance $(y(s)/d_i(s))$ and (b) Output to measurement noise $(y(s)/d_o(s))$ magnitude response plots for PBC (red) and MPBC (black) respectively.

## REFERENCES

S. S. Aphale, A. J. Fleming, and S. O. Reza Moheimani. Integral resonant control of collocated smart structures. *Smart Materials and Structures*, 16(2):439–446, 2007.

S. S. Aphale, B. Bhikkaji, and S. O. R. Moheimani. Minimizing scanning errors in piezoelectric stack-actuated nanopositioning platforms. *IEEE Transactions on Nanotechnology*, 7(1):79–90, 2008.

B. Bhikkaji, M. Ratnam, A. J. Fleming, and S. O. R. Moheimani. High-performance control of piezoelectric tube scanners. *IEEE Transactions on Control Systems Technology*, 15(5 SPEC. ISS.):853–866, 2007.

S. Devasia, E. Eleftheriou, and S. O. R. Moheimani. A survey of control issues in nanopositioning. *IEEE Transactions on Control Systems Technology*, 15(5 SPEC. ISS.):802–823, 2007.

R.C. Dorf and R.H. Bishop. *Modern Control Systems*. Prentice Hall, 2010. ISBN 9780131383104.

J. L. Fanson and T. K. Caughey. Positive position feedback control for large space structures. *AIAA Journal*, 28(4): 717–724, 1990.

A. J. Fleming and A. G. Wills. Optimal periodic trajectories for band-limited systems. *IEEE Transactions on Control Systems Technology*, 17(3):552–562, 2009.

G. C. Goodwin, S. F. Graebe, and M. E. Salgado. *Control System Design*, 2001.

S. O. R. Moheimani. Minimizing the effect of out of bandwidth modes in truncated structure models. *Journal of Dynamic Systems, Measurement and Control, Transactions of the ASME*, 122(1):237–239, 2000.

S. O. R. Moheimani. A survey of recent innovations in vibration damping and control using shunted piezoelectric transducers. *IEEE Transactions on Control Systems Technology*, 11(4):482–494, 2003.

M. Namavar, A. J. Fleming, M. Aleyaasin, K. Nakkeeran, and S. S. Aphale. An analytical approach to integral resonant control of second-order systems. *IEEE/ASME Transactions on Mechatronics*, (in press), 2013. DOI: 10.1109/TMECH.2013.2253115.

M. Namavar, A. J. Fleming, and S. S. Aphale. Resonance-shifting integral resonant control scheme for increasing the positioning bandwidth of nanopositioners. In *12th Bi-annual European Control Conference, ECC 2013, Zurich, Switzerland*, July, 2013.

H. R. Pota, S. O. R. Moheimani, and M. Smith. Resonant controllers for smart structures. *Smart Materials and Structures*, 11(1):1–8, 2002.

Andre Preumont. *Vibration Control of Active Structures : An Introduction (2nd Edition)*. Kluwer Academic Publishers, Secaucus, NJ, USA, 2002 2002. ISBN 9780306484223. ID: 10067232.

M. Ratnam, B. Bhikkaji, A. J. Fleming, and S. O. R. Moheimani. Ppf control of a piezoelectric tube scanner. In *44th IEEE Conference on Decision and Control, and the European Control Conference, CDC-ECC '05*, volume 2005, pages 1168–1173, 2005. ISBN 0780395689 (ISBN); 9780780395688 (ISBN).

S. Salapaka, A. Sebastian, J. P. Cleveland, and M. V. Salapaka. High bandwidth nano-positioner: A robust control approach. *Review of Scientific Instruments*, 73 (9):3232, 2002.

Y. K. Yong, S. S. Aphale, and S. O. R. Moheimani. Design, identification, and control of a flexure-based XY stage for fast nanoscale positioning. *IEEE Transactions on Nanotechnology*, 8(1):46–54, 2009.

Q. Zou, K. K. Leang, E. Sadoun, M. J. Reed, and S. Devasia. Control issues in high-speed afm for biological applications: Collagen imaging example. *Asian Journal of Control*, 6(2):164–178, 2004.